

Active techniques for wind and wave observations: radar altimeter

Saleh Abdalla

*ECMWF
Shinfield Park, Reading, RG2 9AX, UK
abdalla@ecmwf.int*

ABSTRACT

Radar altimeter is a space-borne nadir-looking active instrument that can measure ocean surface wind speed and significant wave height among other parameters. While the wind speed product is not assimilated in the ECMWF atmospheric model, it is invaluable for model verification. Besides the model verification, significant wave height is assimilated at the ECMWF wave model. The impact of wave height data proves to have positive impact on the model analysis and forecasts. Continuous verification and monitoring of altimeter data ensures that the data have good quality and fit for purpose. In principle, the verification and monitoring of satellite data proved to be of mutual benefit for both numerical weather prediction community and the space agencies.

1 Introduction

The radar altimeter is a nadir looking active microwave instrument. This instrument emits pulses, and by measuring the travel time of the return pulse, after extensive corrections for atmospheric delays, and accurate determination of the satellite orbit, for example, information on the mean sea level may be obtained. To a good approximation the backscattered return, which may be described by specular reflection, is inversely proportional to the mean square slope (mss) of the sea surface. As according to Cox and Munk (1954) mean square slope is closely related to the surface wind speed, the radar backscatter is a good measure for wind speed. Finally, the radar altimeter also provides a measure of the significant wave height through the distortion of the mean shape of the return pulse. The earlier return from the wave crests and the retarded return from the wave troughs lead to a deformation of the return pulse which can directly be related to the significant wave height. To determine the mean pulse shape, in the order of one thousand pulses are averaged, yielding one significant wave height measurement about every 7 km along the satellite track. For a Gaussian sea surface, the relation between pulse shape and the root mean square (rms) of the sea surface displacement can be determined theoretically (although there are small corrections needed caused by deviations from normality, cf. Janssen, 2000; Gomez-Enri et al., 2007). This model has been confirmed by numerous comparisons with in situ measurements. Figure 1 shows typical wave form from averaging of about 100 individual returned signals from the ocean surface within one second. The shape of the wave form is used to infer various parameters. The typical accuracy of significant wave height of the older generation of radar altimeters is thought to be the maximum of 0.5 m or 10% of wave height in the range of 1 to 20 m, while the wind speed accuracy is between 1.5 and 2 m s⁻¹ (for wind speed in the range of 0 to 20 m s⁻¹). As will be discussed later based on a triple collocation technique, nowadays the accuracy of significant wave height is thought to be 6% of significant wave height, while the error in wind speed is around 1.0 m s⁻¹.

The radar altimeter is an important component of the payload of a number of satellites such as Seasat, Geosat, ERS-1/2, Topex/Poseidon, GEOSAT-Follow-On (GFO), ENVISAT, Jason-1, Jason-2,

Cryosat-2 and SARAL. For operational models, the data need to be available in near-real time (i.e. within three hours). ERS-1/2, ENVISAT, Jason-1, Jason-2, Cryosat-2 and SARAL provide these fast delivery products. In general two polar orbiting satellites give good coverage in about 6 hours.

Before we start the discussion on the value of altimeter wind speed and wave height data for numerical wave prediction, it should be noted that, on the other hand, wind and wave model products have been quite useful in the validation and calibration of ESA's altimeter wind and wave product. The necessary calibration and validation of a satellite sensor requires large amounts of ground truth which should cover the full range of possible events. In particular the number of reliable wave in situ measurements is very limited and, because of financial restrictions, dedicated field campaigns are possible only at a few sites. In contrast to that, model data are relatively cheap and provide global data sets for comparison. Thus, the combination of both in-situ observations and model data seems to be an optimal cal/val dataset. During the ERS-1/ERS-2 and ENVISAT cal/val campaigns the altimeter-model comparisons have been very effective in identifying errors and problems in the altimeter processing and retrieval algorithms. Few examples can be found in Janssen et al. (2008).

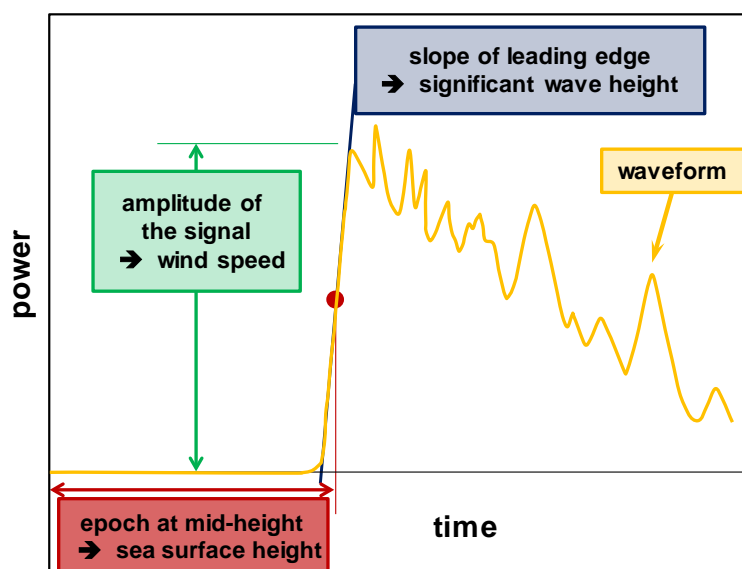


Figure 1: Information extracted from a radar echo reflected from ocean surface (after averaging ~ 100 individual waveforms within $\sim 1/20$ th of a second).

Most of the modern radar altimetry missions carry dual frequency altimeters to estimate the impact of the atmosphere on the radar signal (ionospheric impact). The primary (or the only in the case of mono-frequency altimeters) electromagnetic wave frequency is usually Ku-band which has a wavelength of about 2.5 cm (e.g. ERS-1/2, ENVISAT, Jason-1/2/3, and Sentinel-3). The exception is SARAL which implements the Ka-band with a wavelength of about 0.8 cm. The secondary frequency is mainly the C-band with a wave length of about 5.5 cm (e.g. Topex, Jason-1/2/3 and Sentinel-3). ENVISAT used S-band (wave length of about 9 cm) as the secondary frequency.

Radar altimeters are invaluable instruments to measure the following important parameters:

- Sea surface height (SSH)
- Significant wave height (SWH)
- Surface wind speed
- Ice/land/lakes characteristics

Most of altimetry missions accommodate a microwave radiometer instrument to measure the atmospheric humidity for the purpose of the determination of the impact of atmospheric humidity on the altimeter measurements. The water vapour causes delay of the radar signal which can cause errors in the order of 10's of centimetres. Furthermore, it causes an attenuation which is reflected in wind speed inaccuracies. For longer electromagnetic wave lengths (e.g. Ku- and C-bands) this attenuation is negligible. However, for shorter wave lengths (e.g. Ka-band), the impact is rather high. Additional products like total column water vapour are also available from those microwave radiometers. Typical daily coverage of various altimeters are shown in Figure 2.

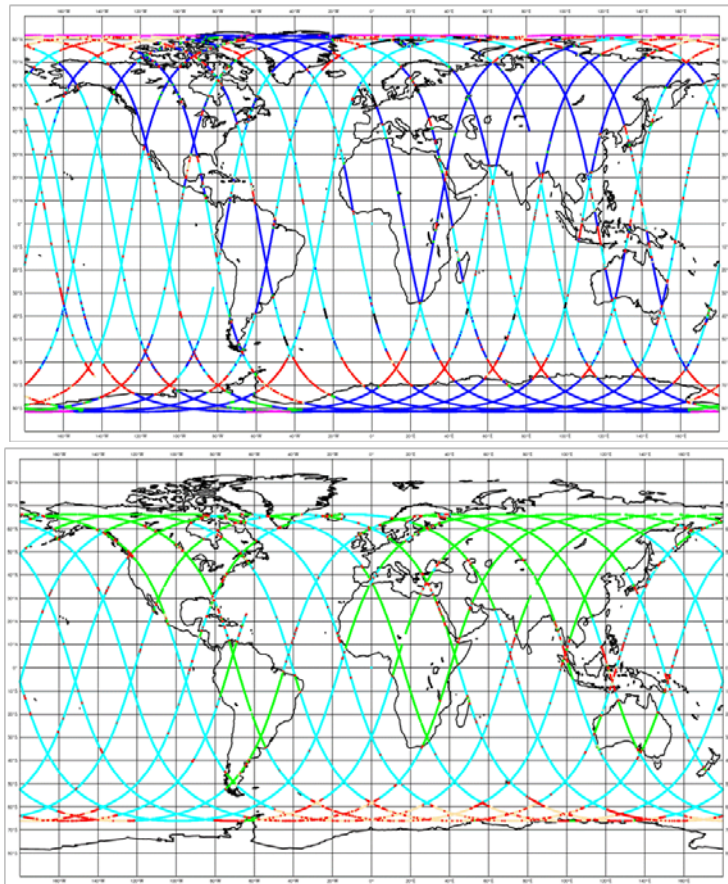


Figure 2: Typical Daily Coverage of Envisat/SARAL family (top) and Jason-1/2 family (bottom).

2 Altimeter Surface Wind Speed

2.1 Principles

Although there is a reasonable correlation between altimeter backscatter (σ_0) and surface wind speed U_{10} , researchers have often wondered whether there are not additional sea state parameters relevant in the relation between backscatter and wind speed. For a nadir-looking radar the main scattering mechanism is specular reflection. Therefore the backscatter is proportional to the joint probability density of slopes $p(\eta_x, \eta_y)$ of the surface η , where η_x and η_y are the slope components in two orthogonal directions. The radar backscatter $\sigma_0(\theta)$ at an incidence angle θ is then given by the classical result (Barrick, 1968; Valenzuela, 1978):

$$\sigma_0(\theta) = \frac{\pi |R(0)|^2}{\cos^4 \theta} p(\eta_x, \eta_y) \Big|_{spec} \quad (1)$$

where $R(0)$ is the Fresnel reflection coefficient for normal incidence and the probability density of slopes $p(\eta_x, \eta_y)$ is evaluated at the specular points. Accordingly, only surface facets normal to the direction of the incident radiation contribute to the backscattering. For small slopes the pdf of the surface slope is given by a Gaussian distribution (Cox and Munk, 1954). For normal incidence ($\theta = 0$), which is the case of altimeters and assuming an isotropic surface with total slope variance of s^2 , (1) reduces to:

$$\sigma_0(\theta) = \frac{|R(0)|^2}{s^2} \quad (2)$$

In order to apply (2) it should be realized that only a portion of the total mean square slopes of the ocean surface is included in s^2 , namely only those ocean waves whose wavenumber ($k=2\pi/\lambda$ with λ being the wavelength) is smaller than the wavenumber of the electromagnetic radiation, k_R . With $F(k, \varphi)$ the ocean surface wave spectrum, where k is the wavenumber and φ the wave propagation direction, the slope variance s^2 therefore becomes:

$$s^2 = \int_0^{k_R} \int_0^{2\pi} k \, dk \, d\varphi \, k^2 F(k, \varphi) \quad (3)$$

Eq. (2) clearly shows how the radar backscatter return depends on the sea state through the mean square slope (mss), s . Traditionally, however, the radar backscatter has been interpreted in terms of the surface wind speed, as Cox and Munk (1954) showed that there is a correlation between mean square slope and surface wind. Nevertheless, the relation between these two parameters is certainly not perfect. Several studies (Monaldo and Dobson, 1989; Glazman and Pilorz, 1990; Glazman and Greysukh, 1993; Lefevre et al., 1994; Hwang et al., 1998; Gourrion et al., 2002) suggest that in the presence of swell the radar backscatter may depend on both the local wind speed and the sea state. Therefore, a number of researchers have made attempts at developing a retrieval algorithm that includes a measure of the sea state. Most authors choose the significant wave height as measure of sea state, because this parameter is readily available from the radar altimeter. Gourrion et al. (2002) have performed the most extensive study in this direction and one of their main results shows the relation between Topex backscatter σ_0 and surface wind speed U_{10} from the NSCAT scatterometer varies with respect to the significant wave height H_s (as obtained from Topex). Their results show that in particular for low wind speeds there is a dependence of the radar backscatter on significant wave height, and a two-dimensional model of the type:

$$U_{10} = f(\sigma_0, H_s) \quad (4)$$

and its inverse was developed using a neural network approach. Gourrion et al (2002) presented clear evidence that, compared to the one-dimensional models such as the MCW retrieval algorithm, the sea-state dependent algorithm (called from now on the Gourrion algorithm) performed better. Consequently, the Jason-1 and Jason-2 altimeter wind speed observations are obtained using this retrieval algorithm. The good performance of the Gourrion algorithm is reflected by the validation efforts at ECMWF where routinely the Jason-1/2 wind speed is compared with analyzed ECMWF wind speed. The typical value for the global scatter index is slightly more than 16% which, with a mean observed wind speed of 8 ms^{-1} , corresponds to a standard deviation of error of 1.25 m s^{-1} .

Nevertheless, one may wonder to what extent the sea state information has resulted in a better wind speed retrieval. For this reason Abdalla (2007 and 2012) improved the pure wind speed algorithm of Chelton and Wentz by using a much larger data set (consisting of both ECMWF winds and in-situ

observations) for fitting the unknown coefficients and this algorithm was introduced for ENVISAT in 2005. Global monitoring the Jason-1 Operational Sensor Data Record products at ECMWF suggests that the Jason Ku-band σ_0 is about 0.4 dB higher than that of ENVISAT. Accordingly, the Jason-1 σ_0 values were reduced by this amount before applying the Abdalla algorithm. It turned out that this algorithm is performing somewhat better than the Gourrion algorithm. A reason for this perhaps counter-intuitive finding may be that the comparison of the results of the Gourrion algorithm with alternative algorithms was not quite fair because the older algorithms were trained on a much smaller data set than the sea state dependent algorithm.

The empirical relations between surface wind speed and the altimeter backscatter σ_0 for Ku-band (as provided by ENVISAT) and Ka-band (as provided by SARAL) are shown in Figure 3. One should keep in mind that the stronger the wind is, the rougher the surface (i.e. the larger the mss) is and therefore the smaller the backscatter is. Note that the relation between the mss and backscatter in the case of altimeter is the inverse of that of the scatterometer (as described by De Chiara, 2015).

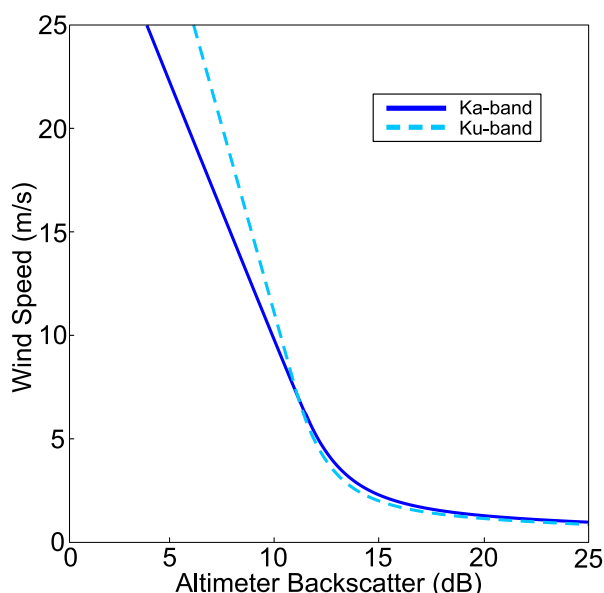


Figure 3: Relation between wind speed and altimeter backscatter

Errors in altimeter surface wind speed are mainly originated from algorithm assumptions, waveform retracking, and various environmental factors that cause unaccounted-for variations to the backscatter. As discussed above, the current altimeter wind speed algorithms either ignore the sea state or use significant wave height as proxy for its impact. Clearly, both choices lack the impact of the sea state. The actual wave forms are usually noisier than that shown in Figure 1. In some cases, they may suffer some kind of distortion. The retracking of those wave forms using an expected shape leads to some errors. The correction for atmospheric attenuation especially for the case of short electromagnetic signals (e.g. Ka-band), which is either based on microwave radiometer measurements or atmospheric model, is not perfect. The impact of other environmental factors (e.g. rain), which are not taken in consideration, contribute to the wind speed errors.

2.2 Verification and Monitoring

Surface wind speed product from altimeters is not assimilated at ECMWF integrated forecasting system (IFS). Instead, it is used for independent verification of the model winds. For example, it is

used to assess various model changes. Therefore, verification of this product and monitoring its quality are very important tasks. An automated system was set up to monitor the availability and the quality of the altimeter wind speed product in near real time (NRT). Currently, altimeter wind speed from Jason-2, Cryosat-2 and SARAL are routinely received and monitored.

The verification of altimeter wind speeds is done against both IFS model analysis and in-situ measurements at few hundreds of offshore buoys and platforms. While the in-situ measurements are widely accepted as the “ground truth” (although there is an increasing evidence using the triple collocation technique that this is not true; cf. Janssen et al., 2007 and Abdalla et al., 2011), the geographical coverage of those in-situ stations is limited to offshore Europe and Northern America and parts of the tropics (denoted by the blue dots in the map shown in Figure 4). On the other hand, the model comparison provides a real global assessment of altimeter wind speed.

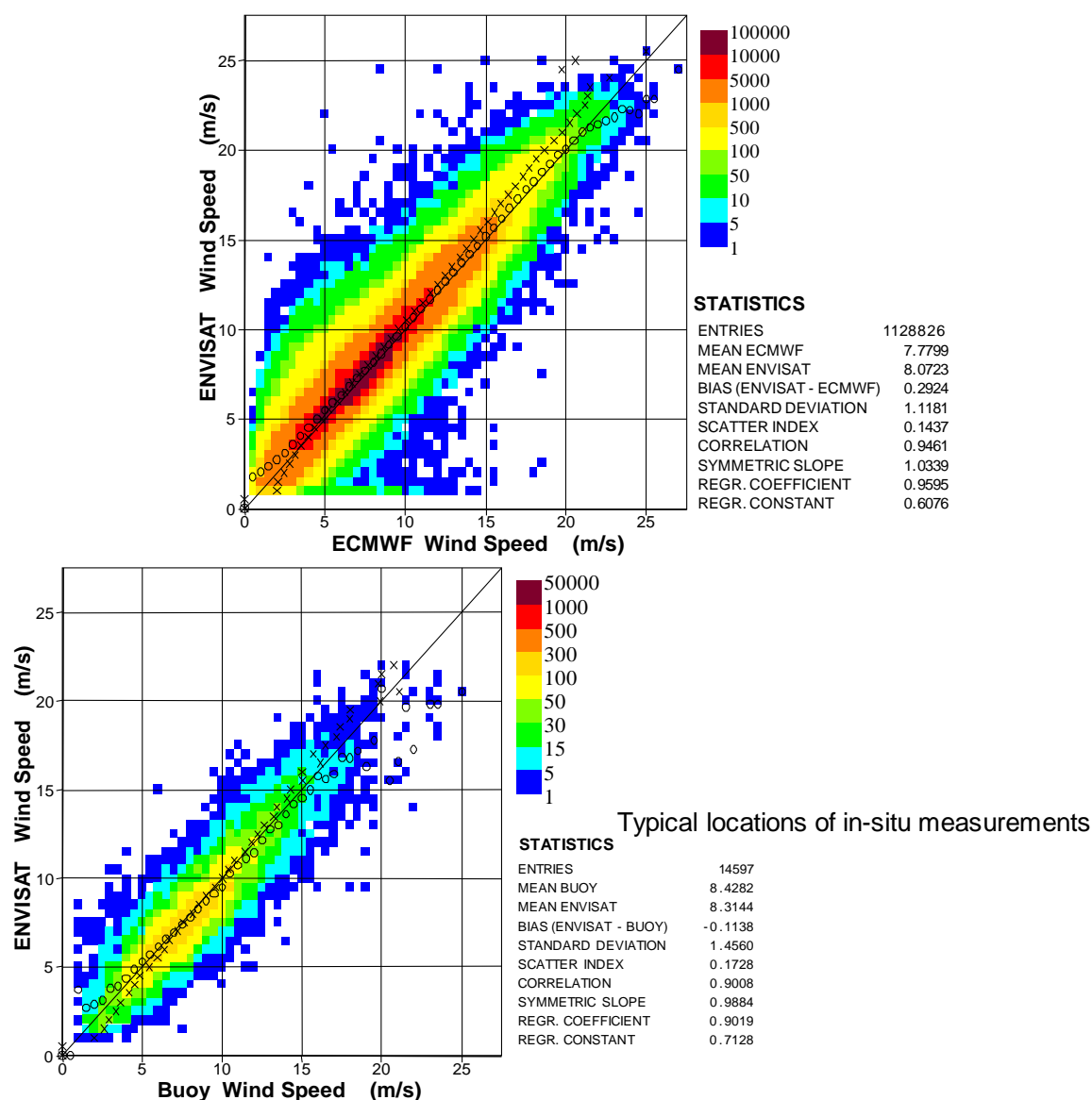


Figure 4: Comparison between ENVISAT NRT wind speed and ECMWF model AN (top) and in-situ measurements (bottom) for all data from 1 Jan. 2011 to 31 Dec. 2011. Typical locations of in-situ measurements are also shown.

For the purpose of altimeter wind speed verification, an in-situ wind speed measurement is only trusted if it is associated with an acceptable significant wave height (SWH) value. Therefore, rejection of wave height in an in-situ record invalidates the wind speed measurement in the same record. In fact the same assumption is used for the quality control of altimeter data.

In general, the NRT altimeter wind speed data compare well with the ECMWF model analysis and the in-situ observations as can be seen in the scatter plots shown in Figure 4. The scatter plots in Figure 4 represent two-dimensional (2-D) histograms showing the number of observations in each 2-D bin of $0.5 \text{ m/s} \times 0.5 \text{ m/s}$ of wind speed. Typically, the standard deviation of the difference (SDD) between altimeter winds and the model or the in-situ winds is slightly above 1.0 m s^{-1} which corresponds to scatter index (SI, defined as the SDD normalised by the mean of the reference which the in-situ or the model AN) values of about 15%.

2.3 Assessment of Model Developments

Compared to the dense geographical coverage of scatterometers with swaths of few hundreds of kilometres, the mesh-like coverage of altimeters (see Figure 2) can be considered as rather limited. Therefore, it was decided at ECMWF not to assimilate altimeter surface wind speed product into IFS. Instead, this product is kept as an independent assessment tool for the model performance and the model developments. For example, Figure 5 shows the global surface wind speed SDD between the ENVISAT RA-2 and ECMWF model. There were two drops in the SDD values, one was due to altimeter processing chain in October 2005 and the second was due a model change in June 2007. However, there was also a slight increase in SDD due to another model change in March 2009. The list of model changes in June 2007 includes the assimilation of ASCAT wind velocity (in fact this was switched on few days after the main model change).

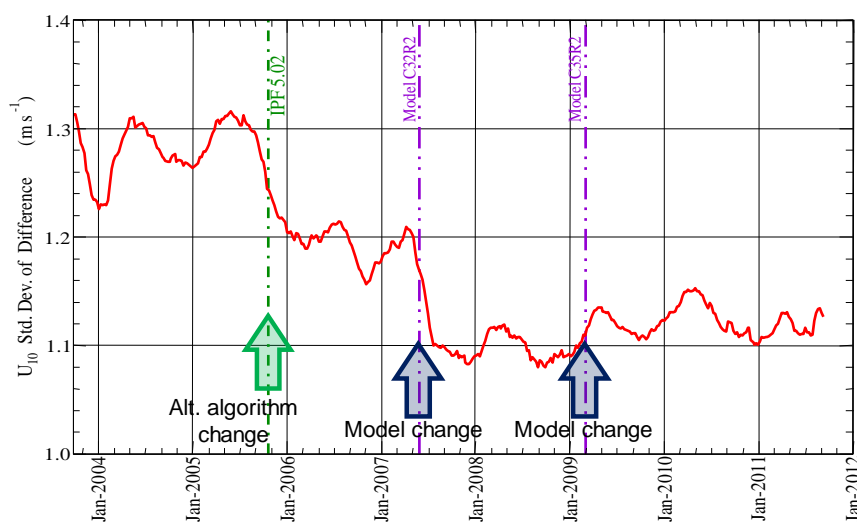


Figure 5: Change assessment: Change of SDD between ENVISAT RA-2 and ECMWF model wind speed.

2.4 Estimation of Effective Model Resolution

Very sharp atmospheric phenomena (e.g. frontal zones or tropical cyclones) with scales of 50–80 km or the equivalent of 3–5 model grid spacings are frequently seen in the forecasts from the ECMWF Integrated Forecasting System (IFS). Since 26 January 2010, the high-resolution forecasts (HRES) use a model with a linear spectral truncation of TL1279 which corresponds to a horizontal grid resolution

of 16 km. However, due to the nature of numerical solutions and parameterizations, the model effective resolution degrades to several grid spacings. It is of interest to estimate this effective resolution.

Abdalla et al. (2013) presented a way to estimate the effective model resolution at the ocean surface by comparing the spectrum of model 10-m wind speed fields against a corresponding spectrum from the independent radar altimeter wind measurements. The restriction to the ocean surface is due to the fact that altimeter wind speed measurements are only possible over the water surface. It is found that the effective useful resolution (defined as the scale at which the model is able to retain 50% of the spectral density) of the current HRES is 3–5 grid spacings supporting the possibility of observing sharp phenomena at this scale. IFS is able to fully resolve scales of about 8 grid spacings as can be seen in Figure 6. In general, all ECMWF model configurations show similar effective resolutions in terms of grid spacings.

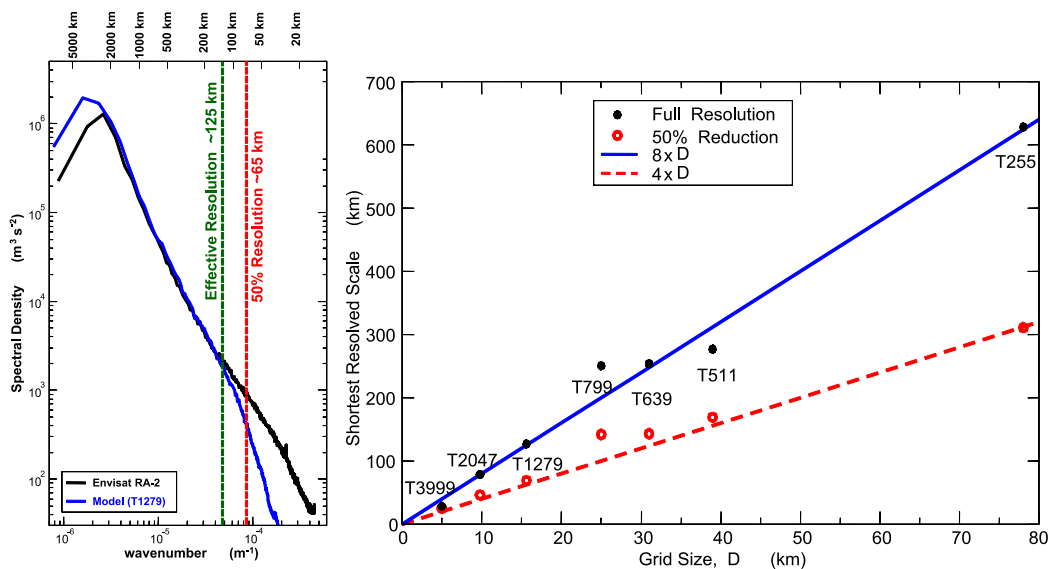


Figure 6: Spectra of ENVISAT altimeter and model 10-m wind speed spectra (left) and effective model resolution of various IFS model configurations (right).

2.5 Random Error Estimation

The triple collocation method to estimate the random errors in three (independent) sources of data was introduced to the meteorological community by Stoffelen (1998). Further improvements and uses have been introduced since then. It is straightforward to show that with three data sets which have uncorrelated errors, the random error of each data type can be estimated from the variances and covariances of the data sets. However, unless additional assumptions are being made, it is not possible to perform an absolute calibration among the data sets, simply because there are not enough equations. A possible way out of this dilemma is to use a minimization procedure. Assume that the random errors are not correlated and that the errors of the three data sets are estimated using the triple collocation method. Given these estimated errors, calibration is then performed using a neutral regression approach based on the minimization of the error in both variants. For an extensive discussion of this approach and a number of applications see Janssen et al. (2007) and Abdalla et al. (2011).

Using the triple collocation method it was possible to estimate the random errors of the ENVISAT, ERS-2, Jason-1 and Jason-2 NRT altimeter SWH and wind speed. In this case, it is emphasized that

Fast delivery products are used which are averaged over a length scale which is compatible with the effective resolution of the ECMWF wave model (~ 75 km). The errors of the model and the buoys are also found. The 10-m wind speed errors are shown Figure 7. The details can be found in Abdalla et al. (2011).

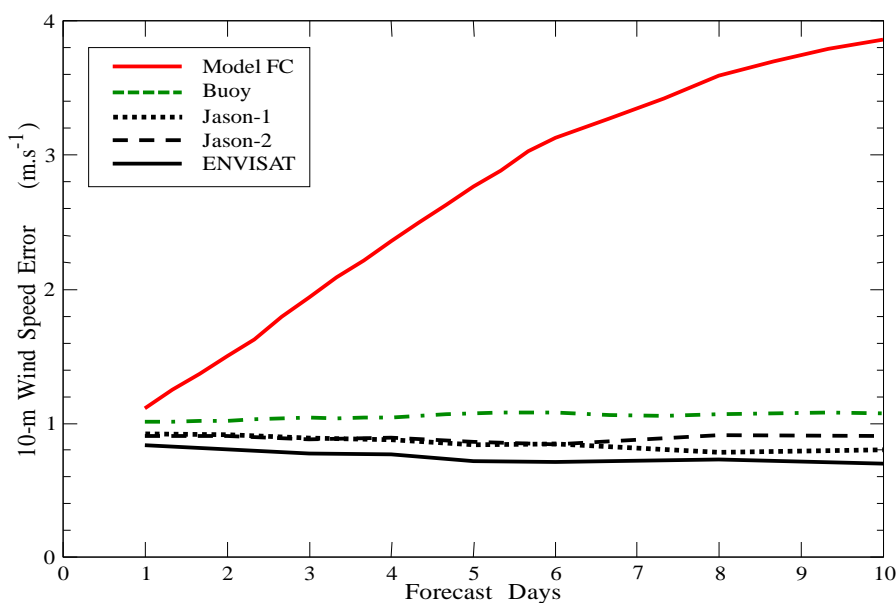


Figure 7: Random error estimation of wind speed using triple collocation technique. Valid in the areas with available in-situ observations (NH) between August 2009 and July 2010.

3 Altimeter Significant Wave Height

3.1 Principle of SWH Measurements

Significant wave height (SWH) is defined as the mean height of highest 1/3 of the surface ocean waves. It is considered as the most important altimeter product as far as the wave prediction is concerned. SWH is used for data assimilation to improve the model analysis and forecast. Therefore, the task of verification and monitoring of SWH is very important.

The temporal variation of the received returned altimeter signal is called the wave form. As shown in Figure 1, there is no received signal during the time when the signal is in its way to and back from the ocean surface. Then a sharp jump, termed here as the “leading edge”, in the received power takes place as most of the signal would arrive back within a short period of time. If the surface reflecting the signal is flat, the jump will be instantaneous. However, the existence of the ocean waves causes the inclination of the leading edge. The higher the SWH is, the more inclined (or the smaller the slope of) the leading edge. This relation between the slope of the wave form leading edge and the SWH is exploited to derive the altimetry SWH product.

SWH product is the most robust altimeter measurement. The errors in the SWH are mainly due to algorithms used for the waveform retracking as the individual wave forms are very noisy. The instrument characterisation is important as incorrect values lead to additional errors.

3.2 Verification and Monitoring of SWH

Verification and monitoring of SWH product is done using the same approach used for surface wind speed (see Section 2.2). However, since altimeter SWH products are usually assimilated in IFS, only model first guess is used for the verification. The same automated system is used to monitor the availability and the quality of the altimeter SWH in NRT. Currently, SWH from Jason-2, Cryosat-2 and SARAL are routinely received and monitored. Jason-2 SWH has been assimilated routinely since 10 March 2009. Cryosat-2 and SARAL SWH products will be assimilated soon.

SWH is compared against in-situ measurements (as done for the wind speed product) and against ECMWF wave model first guess (FG). The model analysis in general cannot be considered as an independent source of data for the verification of altimeter SWH as this product is assimilated by the model. FG fields can be considered of “less dependency” as they contain traces of SWH data assimilated at earlier time windows (not exactly the same data to be verified). Even if SWH product from one of the satellites is not assimilated in the operational model (e.g. Cryosat-2 at the time being), the use of model analysis in the verification is not desirable due to the existence of some degree of dependency through the assimilation of SWH product from other altimeters. All altimeters implement the same method of measurement and share the same algorithms.

In general, the NRT altimeter SWH data compare very well against the ECMWF model FG data and the in-situ observations. Figure 8 shows scatter plots comparing Cryosat-2 NRT SWH products against model FG and in-situ data for the period from 1 April 2013 to 17 June 2014. One needs to remember that the verification against in-situ measurements is limited to the Northern Hemisphere (near the coasts of Europe and North America) and parts of the Tropics while the verification against the model represents a truly global verification. The 2-D histograms in Figure 8 show the number of observations in each 0.25 m x 0.25 m bins of SWH. Typically, the standard deviation of the difference (SDD) between altimeter SWH and the model or the in-situ winds is around 0.25~0.30 m which corresponds to scatter index values of about 10-15%. The bias depends on the instruments but bias correction is applied before data assimilation.

More appropriate method to estimate random errors is the triple collocation technique (Section 2.5). The absolute SWH errors are shown in Figure 9. The details can be found in Abdalla et al. (2011).

3.3 Assimilation of SWH

Unlike atmospheric data assimilation, which started in the 1960's, ocean wave data assimilation emerged only in the 1980's. The prospect of the advent of satellite data encouraged NWP centres to study the possibility of including wave data assimilation schemes in their operational wave forecast suites. For wave analysis, the wind fields are provided from the analysis of the atmospheric model. Satellite wave data are assimilated to improve the initial sea-state used for the wave forecast. This has proved to be of great value (see, e.g. Komen et al., 1994). As an example, Bidlot et al. (2002), Abdalla et al. (2004 and 2011) showed that assimilation of satellite radar altimeter wave heights from ERS-2, ENVISAT, and Jason-2 reduces the model wave height errors with respect to in-situ observations by about 10-20%.

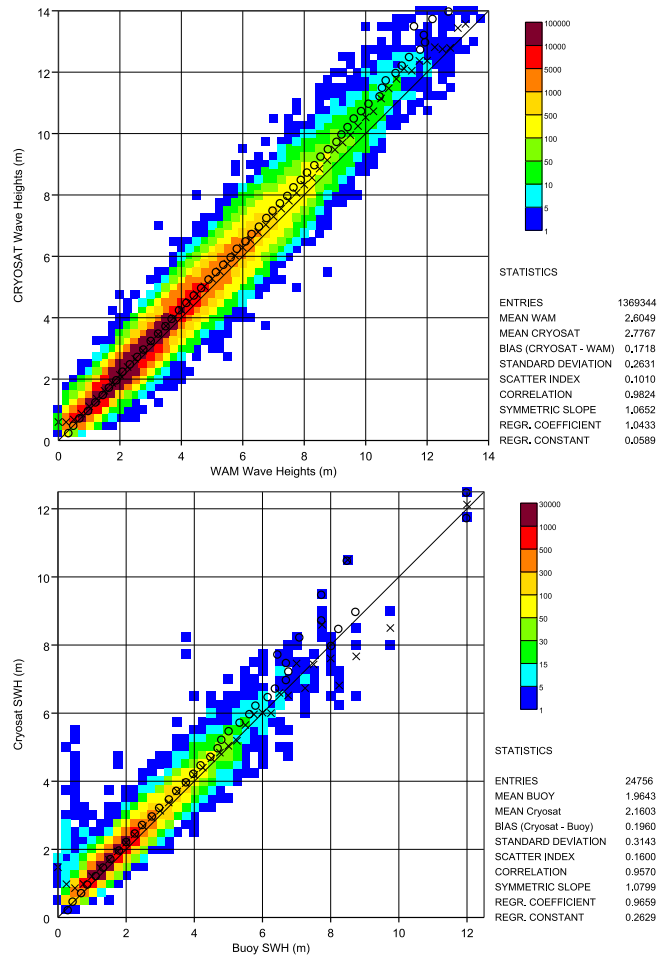


Figure 8: Comparison between Cryosat-2 NRT SWH and ECMWF model FG (top) and in-situ measurements (bottom) for all data between 1 April 2013 and 17 June 2014.

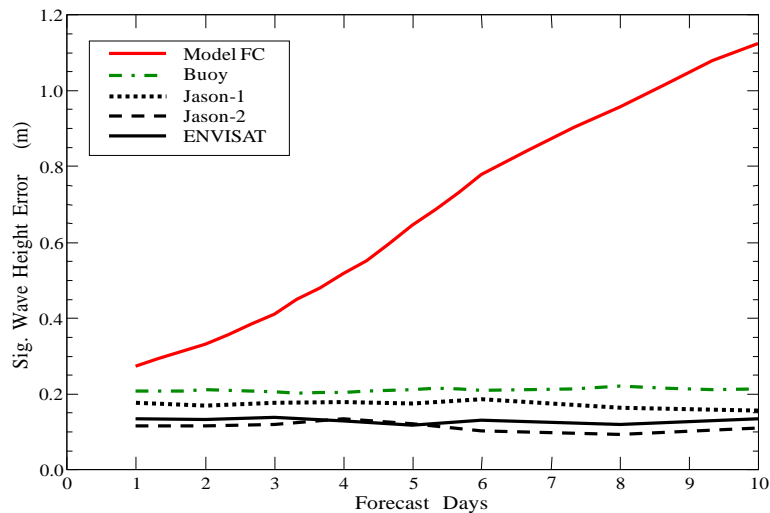


Figure 9: Random error estimation of SWH using triple collocation technique. Valid in the areas with available in-situ observations (NH) between August 2009 and July 2010.

The first operational implementation of SWH assimilation in the global ECMWF IFS was realised on 15 August 1993. The history of ocean wave data assimilation in terms of instruments used is shown in Figure 10.

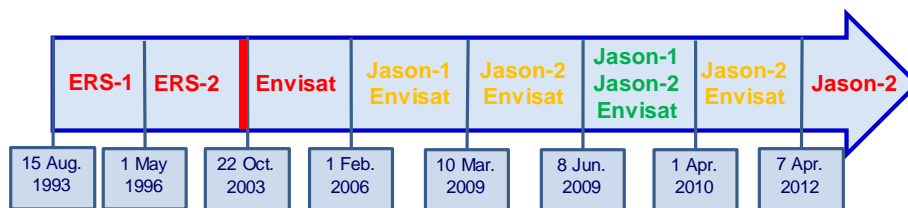


Figure 10: Timeline of altimeter SWH assimilation at ECMWF.

Optimisation procedures are used to find the best or the optimal model state from the model FG and the observations. Assimilation schemes used for wave data analysis can be classified into sequential and variational. The former modifies the model FG to bring them as much as possible towards the observations available within the time-window centred at the analysis time in an independent manner. Such modifications may not be consistent with the model dynamics and may cause some kind of discontinuities. On the other hand, the variational schemes try to find the model solution that minimises the differences with the observations over the whole analysis time window. This implies proper correction to the driving wind fields, which may not be consistent with the atmospheric model dynamics. However, the resulted AN wave fields are consistent with the wave model dynamics. Although variational schemes possess more desirable properties than the sequential schemes, the computational requirements and some practical difficulties like the lack of up-to-date wave-model adjoint prevent them from being used in global operational wave forecasting systems. Furthermore, the main source of error in ocean wave data assimilation is the distribution of SWH analysis increments on the whole wave spectrum which is currently done with several approximations due to the lack of other alternatives.

The optimal interpolation (OI) technique is one of the simplest sequential data assimilation methods. This technique is used at ECMWF (c.f. Lionello et al., 1992) for the assimilation of satellite wave data from altimeters (ERS-1/2, Envisat and Jason-1/2) and from SAR (ERS-2 and Envisat). In the case of altimeter data, the full description of the wave energy, or the wave spectrum, is not available. Only SWH is available. In the model, SWH is a prognostic parameter that is only computed from the full wave spectrum for the output. Therefore, the SWH measurements together with FG SWH are blended using the OI scheme to create an AN SWH field. The AN SWH field together with the model wave growth laws are used to construct the AN spectra by resizing and reshaping the FG spectra. This, of course, implies plenty of assumptions as can be found in Lionello et al. (1992).

Altimeter SWH data go through a quality control process (see, e.g. Abdalla and Hersbach, 2006 and Bauer and Staabs, 1998) involving super-obbing (i.e. producing super-observations by averaging of 11-13 consecutive measurements covering a length of about 75 km). All wrong, noisy and questionable measurements are discarded. Bias correction is applied to harmonise the altimeter data with the model counterparts. The OI scheme is applied to the SWH. The analysis increments are translated into adjustments to the wave spectrum by shifting and scaling the model spectrum based on ocean wave growth laws (for wind-sea dominated conditions) or conservation of wave slope (for the swell dominated conditions)

Figure 11 shows the mean difference between the model analysis from two assimilation experiments covering the period between 14 February and 30 April 2014. The first experiment is a model run assimilating both Cryosat-2 and Jason-2 SWH at the same time after bias correction. The second experiment is another model run assimilating only Jason-2 SWH after bias correction. It is clear that the Cryosat-2 data work towards calming the wave field in the Southern Hemispheric (SH) extra-tropics (latitudes lower than -20°) and increasing the waves in the Northern Hemispheric (NH) extra-tropics (latitudes higher than 20°) and in the tropics (latitudes between 20°S and 20°N).

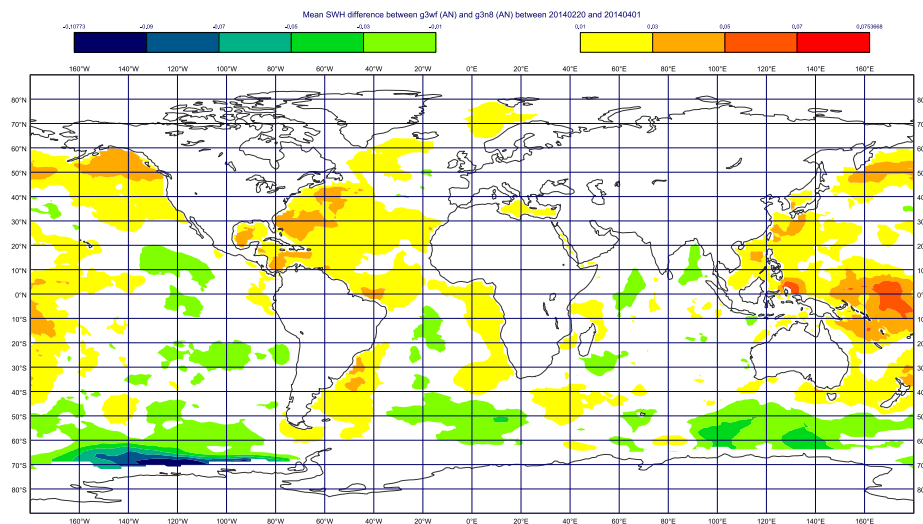


Figure 11: Mean impact of assimilating Cryosat-2 SWH (with BC) on SWH analysis expressed as the difference between a model run assimilating both Cryosat-2 and Jason-2 SWH at the same time and another model run assimilating only Jason-2 SWH.

The assimilation impact can be better assessed using the independent in-situ data. Figure 12 shows the impact of altimeter SWH data assimilation on the model SWH analysis (AN) and forecasts (FC) for several stand-alone high resolution experiments against the model run without data assimilation. The SDD between the model (AN and FC) and the independent in-situ measurements for the model run with data assimilation (SDD_{assim}) and that without data assimilation (SDD_{none}). The random error reduction is computed as the difference between SDD_{none} and SDD_{assim} normalised by SDD_{none} (then multiplied by 100 to get the percentage).

At analysis time, the model run with Jason-2 SWH data assimilation (mimics the current operational system) reduces the model SWH errors by about 3.5% in the extra-tropics and about 5% in the tropics as can be seen in Figure 12. In the extra-tropics, the reduction decreases to almost zero on the third day in the forecast while it retains a small impact of about 0.5% after more than 5 days. Assimilating SWH from other altimeters (SARAL and Cryosat-2) in addition to Jason-2 SWH results in more SWH error reduction (~6.5% and ~9% for extra-tropics and tropics, respectively) at the analysis and slightly more error reduction in the short forecast. Further examples for the SARAL impact can be found in Abdalla (2015).

Clearly, forecast impact of data assimilation is much larger and longer lasting in the areas where swell systems (which give a long memory to the forecast system because their lifetime is large) dominate and where there are significant systematic errors; e.g. tropical areas.

In general, the assimilation of altimeter SWH also has positive impact on the wave spectrum and other integrated wave parameters like the mean wave period which is another important wave parameter (not shown).

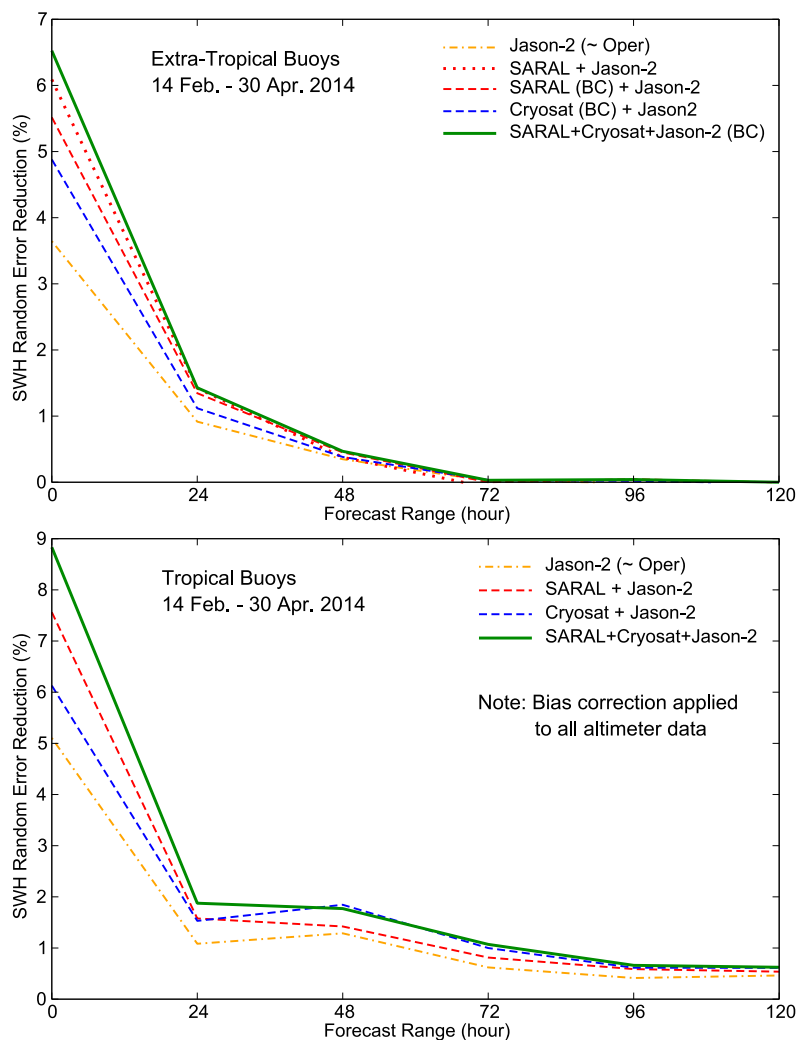


Figure 12: Impact of assimilating altimeter data on SWH random error as verified against NH extra-tropical (top) and tropical (bottom) in-situ data.

The results from the full IFS assimilation experiment using bias-corrected SARAL and Jason-2 SWH and the similar experiment that assimilates only Jason-2 SWH were further verified using Cryosat-2 SWH (the latter was not assimilated). The impact was slightly positive at all regions. As an example, Figure 13 shows the impact of using bias-corrected SARAL SWH data on the SWH bias, SDD and the correlation coefficient with respect to Cryosat-2 SWH in the extra-tropical SH for the period from 14 February to 31 March 2014. The slight positive impact, especially in the short forecast range, is very clear.

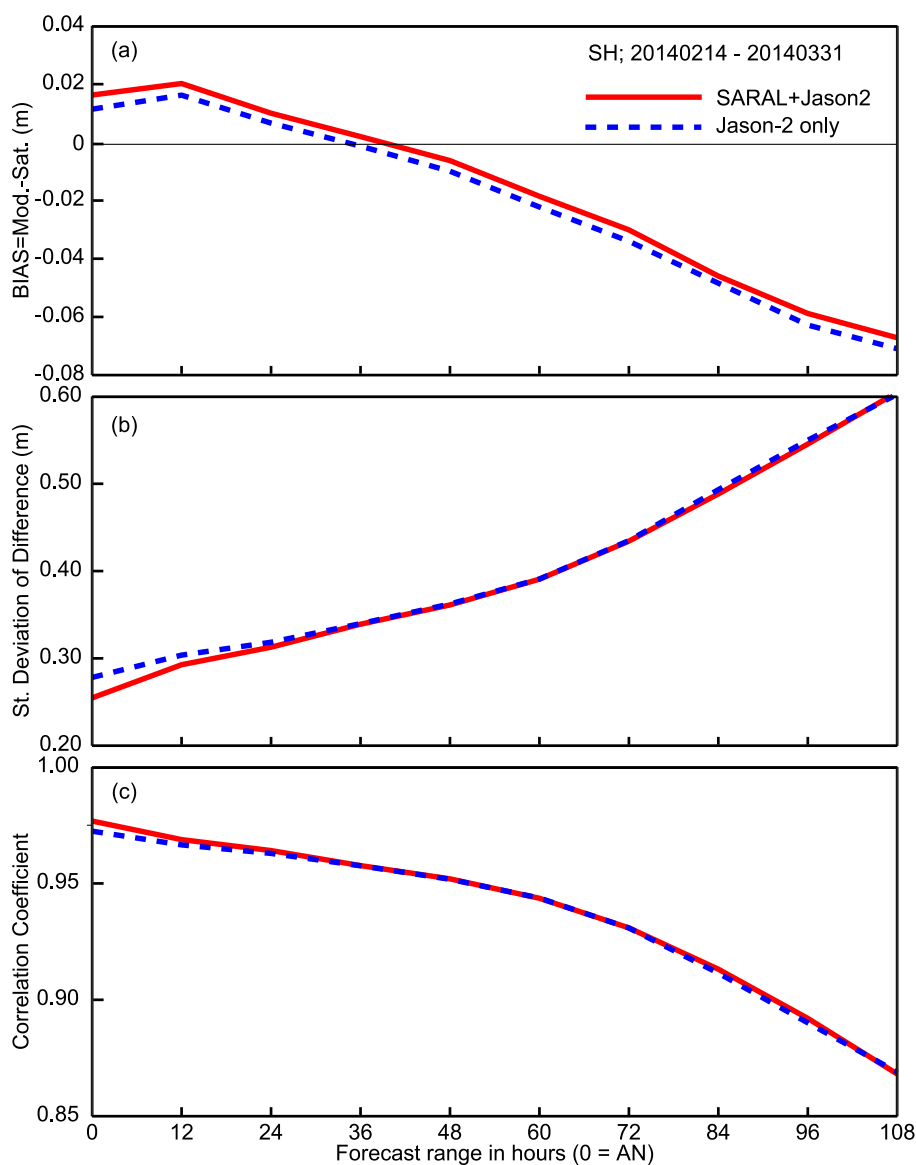


Figure 13: Impact of assimilating SARAL data on SWH error as verified against Cryosat-2 SWH, February – March 2014.

The tight two-way coupling between the atmospheric and ocean wave models within IFS requires that any wave model change including data assimilation does not introduce any degradation to the atmospheric fields. As an example, Figure 14 shows the mean impact of assimilating bias-corrected SARAL SWH in addition to Jason-2 SWH on the anomaly correlation (which is a standard statistic used in numerical weather prediction field and represents the correlation of the model deviations from the climate) of the model 500 hPa geopotential height forecast in the NH and the SH extra-tropics (latitudes higher than 20°) with respect to operational analysis for the period from 14 February to 1 April 2014. Positive values in Figure 10 indicate positive impact and vice versa. It is clear that the impact is almost neutral in terms of statistical significance at 95% level with a tendency towards positive impact in the NH.

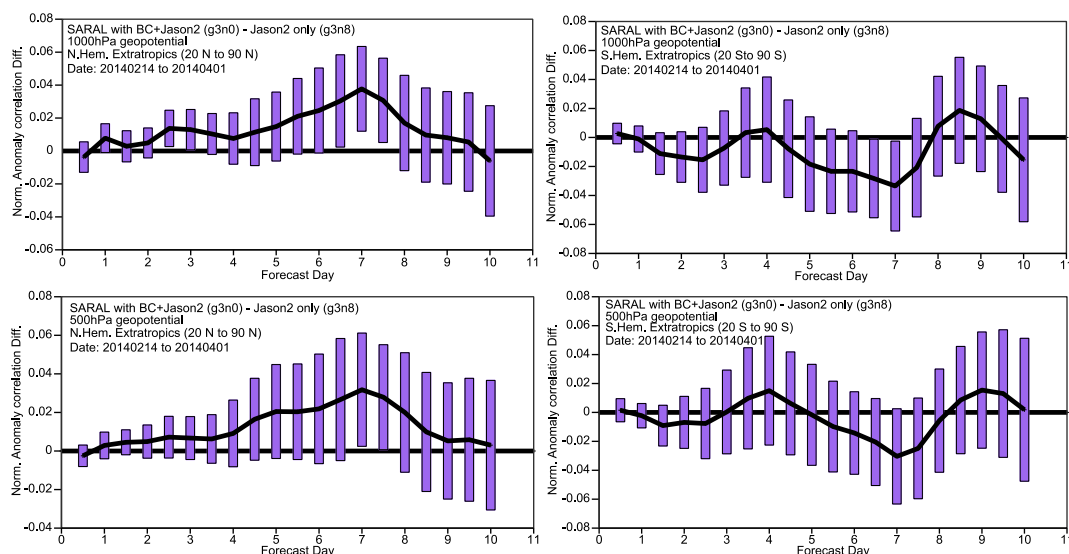


Figure 14: Mean Impact of using SARAL (with BC) SWH on Geopotential anomaly correlation at 1000 hPa (top row) and 500 hPa (bottom row) in the extra-tropical Northern Hemisphere (left column) and the extra-tropical Southern Hemisphere (right column). Vertical bars show the 95% level.

4 Conclusions

NRT radar altimeter products, especially the surface wind speed and the significant wave height, are very useful for ocean-wave related activities. They are used at ECMWF for:

- data assimilation (significant wave height and sea surface height anomaly);
- validation of model analysis and forecasts;
- monitoring of model performance (anomalies, random errors, and effective resolution); and
- assessment of model changes.

In order to achieve the tasks above, the satellite data need to be well calibrated and to be routinely monitored. This is done through the comparison against model products as well as available in-situ observations. As a result, good understanding of the characteristics and the quality of the satellite data is obtained. Routine monitoring also enables the detection of any data anomalies. Both of which are very useful not only for ECMWF but also for the space agencies that provide the data. This 2-way interaction between model and satellite data has been always invaluable for both NWP community and the space agencies.

Acknowledgements

Most of the results shown here were produced within the framework of a series of ESA contracts entitled “the technical support for global validation of Envisat data products”. Data used were provided mainly by ESA, CNES, EUMETSAT and NOAA. The support of Peter Janssen and Jean Bidlot is highly appreciated.

References

Abdalla, S., 2007: Ku-band radar altimeter surface wind speed algorithm. *ECMWF Tech. Memo. No. 524*, Apr. 2007, ECMWF, Reading, UK, 16 pp.,

- Abdalla, S., 2012: Ku-Band Radar Altimeter Surface Wind Speed Algorithm. *Marine Geodesy*, **35:sup1**, 276–298.
- Abdalla, S., 2013: Calibration of SARAL/AltiKa Wind Speed. *IEEE Geosci. Remote Sens. Lett.*, **11**, 1121–1123.
- Abdalla, S., 2013: Global validation of ENVISAT wind, wave and water vapour products from RA-2, MWR, ASAR and MERIS (2011-2012). *ESA Cont. Report 21519/08/I-OL*, ECMWF, Reading, 48 pp.
- Abdalla, S., 2015: SARAL/AltiKa wind and wave products: Monitoring, validation and assimilation, *Marine Geodesy*, in press.
- Abdalla, S. and Hersbach, H., 2006: The technical support for global validation of ERS wind and wave products at ECMWF. *Final report for ESA contract 18212/04/I-OL*, ECMWF, Reading.
- Abdalla, S., Bidlot, J.R., Janssen, P., 2004: Assimilation of ERS and ENVISAT wave data at ECMWF. *Proc. 2004 Envisat & ERS Symposium*, 6–10 Sep. 2004, Salzburg, ESA Proc. SP-572 (CD).
- Abdalla, S., Janssen, P.A.E.M., Bidlot, J.B., 2011: Altimeter Near Real Time Wind and Wave Products: Random Error Estimation. *Marine Geodesy*, **34:3-4**, 393–406.
- Abdalla, S., Isaksen, L., Janssen, P. A. E. M. and Wedi, N., 2013: Effective Spectral Resolution of ECMWF Atmospheric Forecast Models, *ECMWF Newsletter No. 137*, 19–22.
- Barrick, D. 1968: Rough surface scattering based on the specular point theory., *IEEE Trans. Antennas Propagat.*, **16(4)**, 449–454.
- Bauer, E. and Staabs, C., 1998: Statistical properties of global significant wave heights and their use for validation. *J. Geophys. Res.*, **103**, 1153–1166.
- Bidlot, J.R., Holmes, D.J., Wittmann, P.A., Lalbeharry, R., and Chen, H.S., 2002: Intercomparison of the performance of the operational wave forecasting systems with buoy data. *Wea. Forecasting*, **17**, 287–310.
- Cox, C.S. and Munk, W.H., 1954: Statistics of the sea surface derived from sun glitter. *J. Marine Res.*, **13**, 198–227.
- De Chiara, G., 2015: Active techniques for wind observations: scatterometer. In *Proc. Seminar on Use of Satellite Observations in Numerical Weather Prediction*, 8–12 Sep. 2014 (this volume).
- Glazman, R. and Pilorz, S., 1990: Effects of sea maturity on satellite altimeter measurements of surface wind. *J. Geophys. Res.*, **95**, 2857–2870.
- Glazman, R. and Greysukh, A., 1993: Satellite altimeter measurements of surface wind. *J. Geophys. Res.*, **98**, 2475–2483.
- Gómez-Enri, J., Gommenginger, C.P., Srokosz, M.A., and Challenor, P.G., 2007: Measuring Global Ocean Wave Skewness by Retracking RA-2 Envisat Waveforms. *J. Atmos. Oceanic Technol.*, **24**, 1102–1116.
- Gourrion, J., Vandemark, D., Bailey, S., Chapron, B., Gommenginger, G. P., Challenor, P. G., and Srokosz, M. A., 2002: A two-parameter wind speed algorithm for Ku-band altimeters., *J. Atmos. Oceanic Technol.*, **19**, 2030–2048.

- Hwang, P.A., Teague, W.J., Jacobs, G.A. and Wang, D.W., 1998: A statistical comparison of wind speed, wave height and wave period derived from altimeters and ocean buoys in the Gulf of Mexico region. *J. Geophys. Res.*, **103**, 10 451–10 468.
- Janssen, P.A.E.M., 1991: Quasi-linear theory of wind wave generation applied to wave forecasting, *J. Phys. Oceanogr.*, **21**, 1631–1642.
- Janssen, P.A.E.M., 2000: ECMWF wave modelling and satellite altimeter wave data. In Halpern D. (Ed.), *Satellites, Oceanography and Science*, Elsevier Science BV, 35–56.
- Janssen, P.A.E.M., 2004: *The Interaction of Ocean Waves and Wind*, Cambridge University Press, Cambridge, U.K., 300+viii pp.
- Janssen, P.A.E.M., Lionello, P., Reistad, M. and Hollingsworth, A., 1989: Hindcasts and data assimilation studies with the WAM model during the Seasat period. *J. Geophys. Res.*, **C94**, 973–993.
- Janssen, P.A.E.M., Abdalla, S., Hersbach, H. and Bidlot, J.-R., 2007: Error estimation of Buoy, Satellite and Model Wave Height Data. *J. Atmos. Ocean. Technol.*, 1665–1677.
- Janssen, P.A.E.M., Abdalla, S., Aouf, L., Bidlot, J.-R., Challenor, P., Hauser, D., Hersbach, H., Lefevre, J.-M., Vandemark, D., Queffeuou, P. and Quilfen, Y., 2008: 15 years using altimeter sea state products. *ECMWF Tech. Memo. No. 552*, ECMWF, Reading, UK, 37 pp.
- Komen, G.J., Cavaleri, L., Donelan, M., Hasselmann, K., Hasselmann, S., and Janssen, P.A.E.M., 1994: *Dynamics and Modelling of Ocean Waves*, Cambridge Univ. Press, Cambridge, UK, 532 p.
- Lefevre, J., Barckicke, J. and Menard, Y., 1994: A significant wave height dependent function for TOPEX/Poseidon wind speed retrieval. *J. Geophys. Res.*, **99**, 25035–25046.
- Lionello, P., Gunther, H. and Janssen, P.A.E.M., 1992: Assimilation of altimeter data in a global third generation model. *J. Geophys. Res.*, **C97**, 14453–14474.
- Monaldo, F. and Dobson, E., 1989: On using significant wave height and radar cross section to improve radar altimeter measurements. *J. Geophys. Res.*, **94**, 12 699–12 701
- Stoffelen, A., 1998: Error modeling and calibration: Towards the true surface wind speed. *J. Geophys. Res.*, **103**, 7755–7766.
- Valenzuela, G. R., (1978): Theories for the interaction of electromagnetic and oceanic waves - A review. *Boundary-Layer Meteorol.*, **13(1-4)**, 61–85.